

Tissue-dependent mechanosensing by cells derived from human tumors

Kshitiz Parihar¹, Jonathan Nukpezah², Daniel V Iwamoto³, Katrina Cruz³, Fitzroy J Byfield³, LiKang Chin³, Maria E Murray³, Melissa G Mendez³, Anne S van Oosten³, Anne Herrmann³, Elisabeth E Charrier³, Peter A Galie³, Megan Donlick³, Tongkeun Lee³, Paul A Janmey^{2,3,4}, Ravi Radhakrishnan^{1,2}

¹Department of Chemical and Biomolecular Engineering, School of Engineering and Applied Science, University of Pennsylvania, Philadelphia, PA, USA

²Department of Bioengineering, School of Engineering and Applied Science, University of Pennsylvania, Philadelphia, PA, USA

³Institute for Medicine and Engineering, University of Pennsylvania, Philadelphia, PA, USA

⁴Department of Physiology, Perelman School of Medicine, University of Pennsylvania, Philadelphia, PA, USA

Table 1: Number of spread area, aspect ratio, and circularity measurements for each cell line-substrate combination.

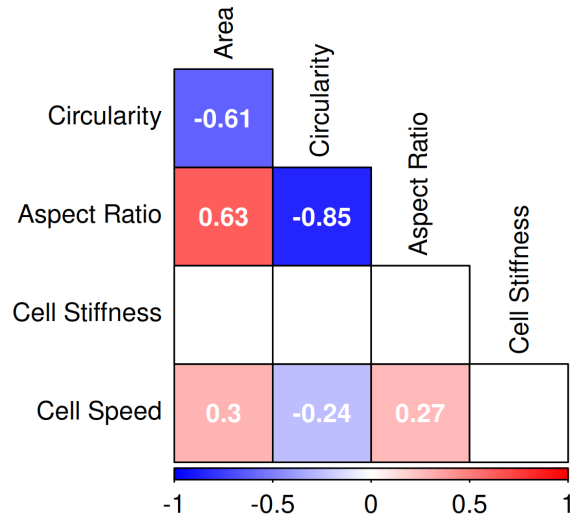
	30kPa Coll	30kPa FN	500Pa Coll	500Pa FN	Glass	HA Coll	HA FN
SK-MEL-2	100	100	101	100	100	101	100
A375	100	100	101	100	100	100	100
WM266-4	100	100	100	100	100	100	100
MeWo	50	50	100	96	100	100	80
RWPE-1(N)	102	103	100	103	100	101	101
22Rv1	99	100	99	81	103	103	98
LnCaP	41	49	34	59	90	32	46
DU145	77	99	67	101	81	102	103
PC-3	101	100	100	90	100	100	40
hTERT-HPNE(N)	94	100	106	97	100	77	76
Panc-1	100	102	72	21	101	103	105
Capan-1	105	100	102	100	101	101	100
SKOV-3	108	101	82	104	102	100	92
Caov-3	85	34	37	16	81	59	43
OVCAR-3	100	86	94	89	90	100	97
NL20(N)	168	257	247	284	248	126	150
NCI-H2126	100	100	100	100	100	100	100
NCI-H2087	100	100	100	100	100	100	100
HCT116	100	100	107	101	101	100	100
HT29	82	55	93	40	165	95	49
SW480	100	100	100	100	100	100	100
SW620	101	100	100	100	101	100	100
hTERT-HME1(N)	100	100	101	100	100	74	51
MCF10A(N)	100	100	100	100	91	88	62
T-47D	100	100	100	86	100	84	97
MCF7	100	68	100	82	100	45	29
MDA-MB-231	121	218	145	164	193	77	160
HCC1937	100	100	100	100	100	100	100
U-87	101	101	102	100	101	101	100
T98G	100	101	100	101	101	100	101

Table 2: Number of cell stiffness measurements for each cell line-substrate combination.

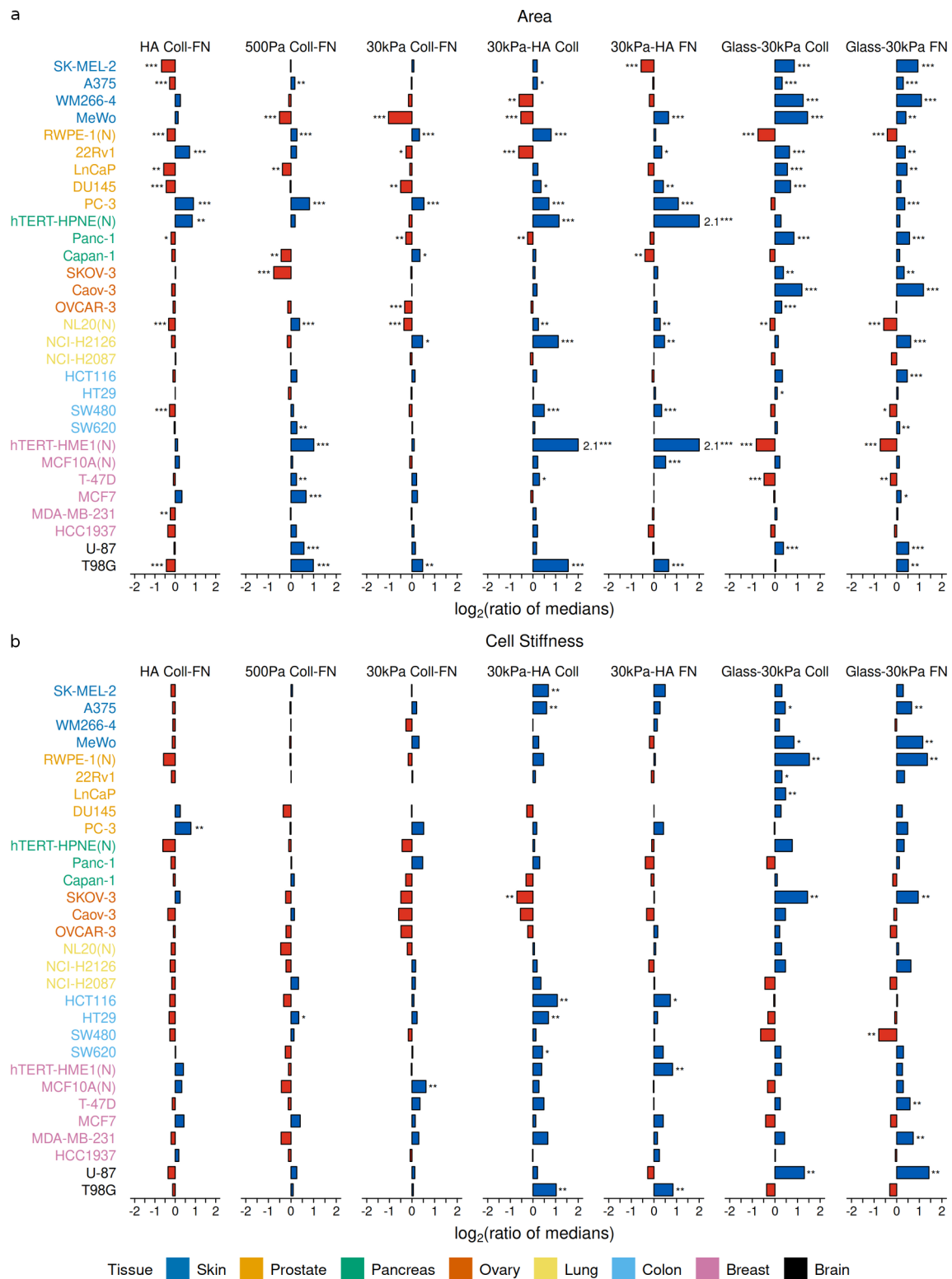
	30kPa Coll	30kPa FN	500Pa Coll	500Pa FN	Glass	HA Coll	HA FN
SK-MEL-2	45	44	43	47	45	50	43
A375	45	30	39	44	45	42	48
WM266-4	63	44	42	41	44	41	48
MeWo	29	31	30	33	30	33	30
RWPE-1(N)	30	36	43	48	67	45	30
22Rv1	30	30	45	30	45	42	30
LnCaP	29	15	27	12	48	0	38
DU145	47	44	51	51	49	41	50
PC-3	45	39	35	29	45	30	28
hTERT-HPNE(N)	45	49	50	42	45	45	45
Panc-1	36	43	30	39	45	43	44
Capan-1	44	31	29	27	33	32	29
SKOV-3	44	39	29	27	28	30	26
Caov-3	44	45	44	45	45	44	28
OVCAR-3	45	44	45	44	46	47	45
NL20(N)	30	30	30	33	33	30	32
NCI-H2126	30	45	29	30	30	30	30
NCI-H2087	30	29	32	30	30	51	30
HCT116	65	45	49	42	67	66	54
HT29	45	39	45	32	45	45	48
SW480	44	53	45	59	63	45	45
SW620	31	29	45	32	31	30	48
hTERT-HME1(N)	45	45	30	47	47	27	45
MCF10A(N)	45	44	44	45	60	45	45
T-47D	48	44	45	45	48	39	42
MCF7	52	42	47	42	29	45	45
MDA-MB-231	45	45	30	30	32	30	45
HCC1937	42	30	45	44	39	42	42
U-87	51	35	59	54	72	54	45
T98G	63	64	59	61	61	57	56

Table 3: Number of cell speed measurements for each cell line-substrate combination.

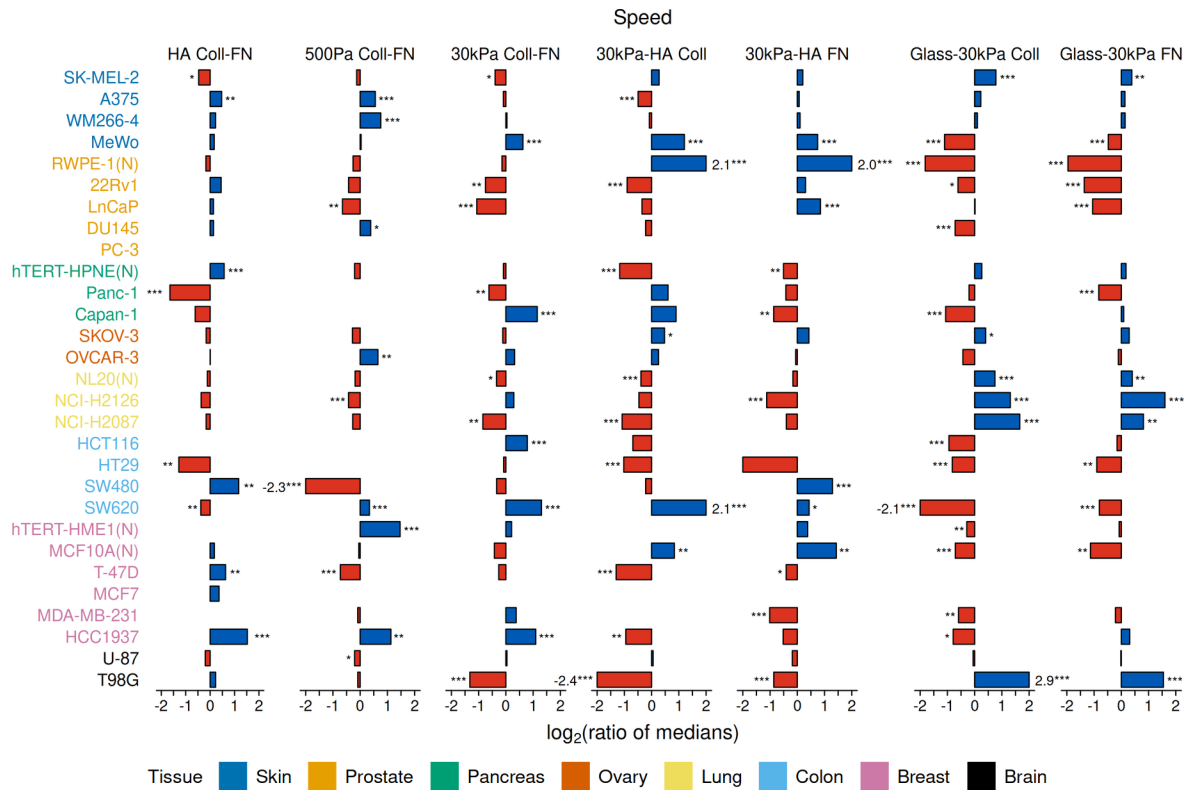
	30kPa Coll	30kPa FN	500Pa Coll	500Pa FN	Glass	HA Coll	HA FN
SK-MEL-2	71	72	61	141	129	70	68
A375	50	50	50	50	51	52	51
WM266-4	41	46	54	51	50	51	51
MeWo	176	58	255	53	159	30	72
RWPE-1(N)	119	109	114	102	66	108	105
22Rv1	36	42	50	45	48	50	56
LnCaP	48	50	29	50	50	48	53
DU145	41	11	27	43	32	50	39
PC-3	13	21	13	99	101	24	14
hTERT-HPNE(N)	55	52	51	51	52	47	50
Panc-1	45	44	33	8	57	62	55
Capan-1	52	46	79	17	56	53	30
SKOV-3	33	26	39	49	51	62	44
OVCAR-3	29	52	49	53	58	51	50
NL20(N)	61	70	54	67	26	45	44
NCI-H2126	51	56	72	75	85	56	103
NCI-H2087	87	27	103	114	104	93	69
HCT116	47	36	44	9	70	26	23
HT29	50	36	57	15	50	50	50
SW480	56	50	55	83	0	40	65
SW620	25	25	51	51	25	51	36
hTERT-HME1(N)	51	29	50	54	52	20	32
MCF10A(N)	50	50	50	60	50	50	52
T-47D	30	56	31	46	14	81	27
MCF7	22	15	37	3	50	50	36
MDA-MB-231	27	25	30	29	34	12	26
HCC1937	51	49	54	50	50	53	48
U-87	59	54	52	102	70	58	47
T98G	74	82	123	94	62	75	86



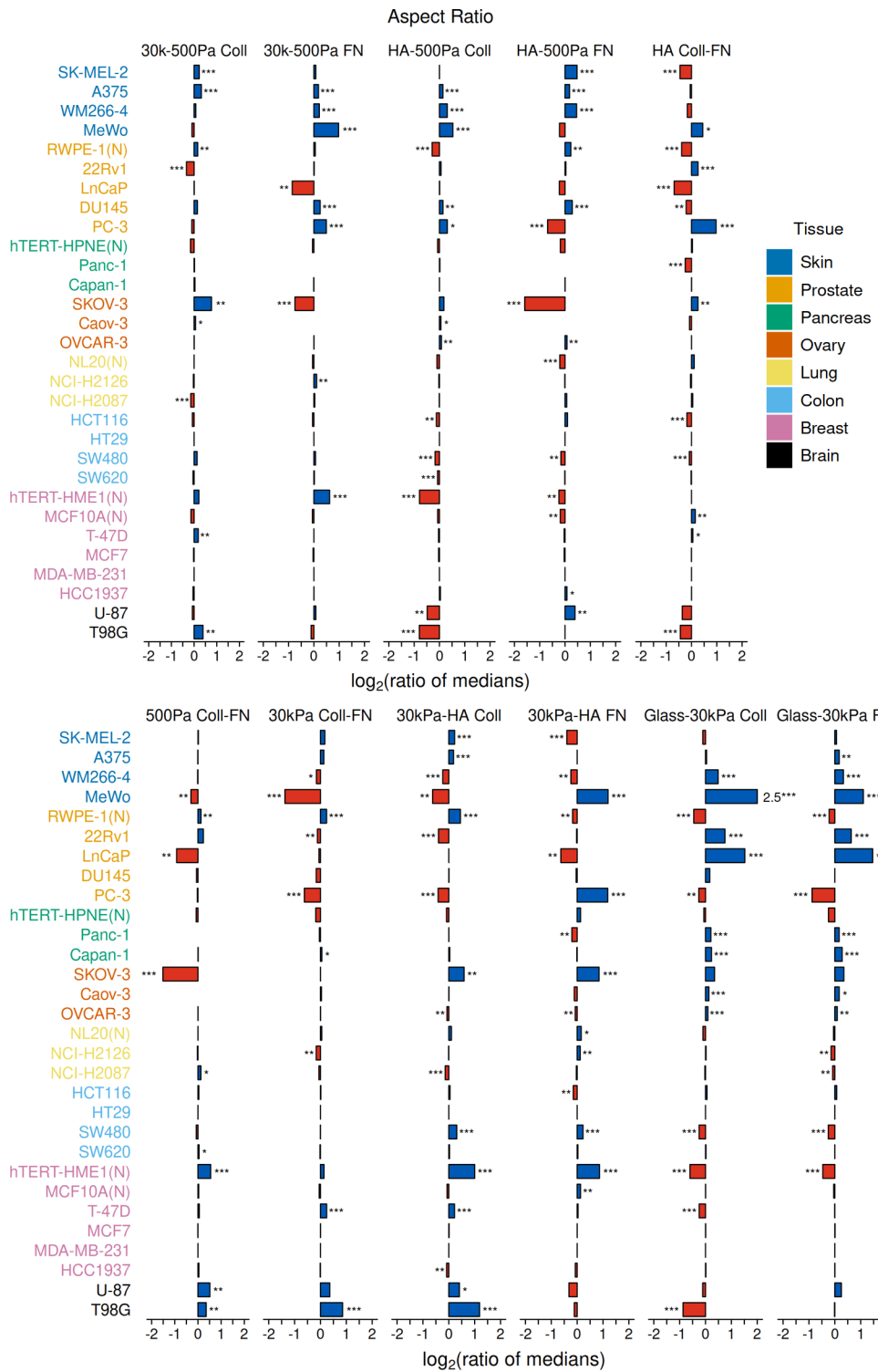
Supplementary Figure 1: Spearman correlation matrix using the median values of the phenotypic features for the cell line-substrate pairs. Only statistically significant correlations are shown. Note that in this analysis only those cell line-substrate pairs are considered which have at least 25 data points for each of the physical feature.



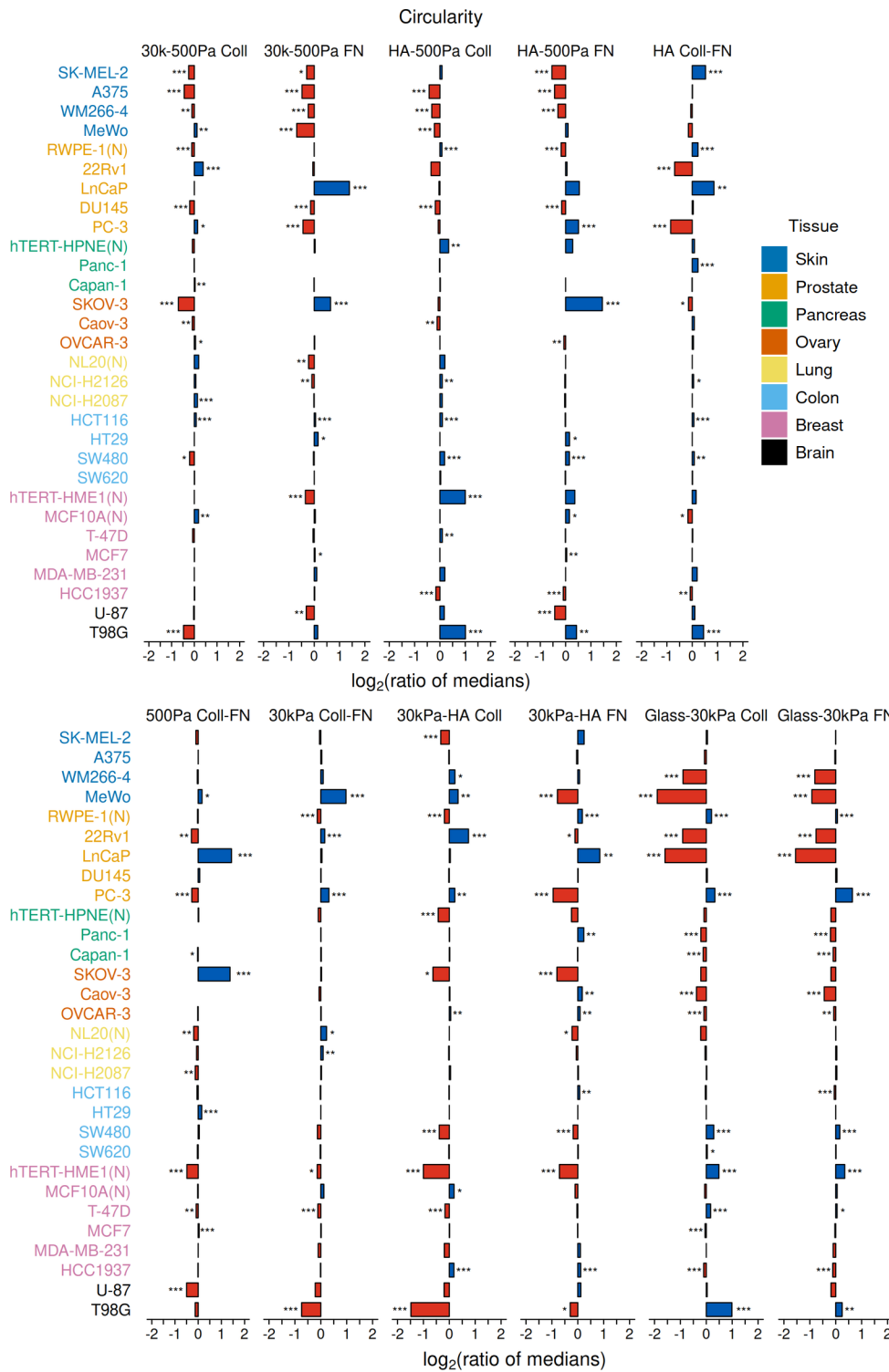
Supplementary Figure 2: For each cell line, the ratio of the median values for (a) area and (b) cell stiffness as a measure of the phenotypic sensitivity to substrate change. (HA Coll-FN: HA Coll/HA FN, 500Pa Coll-FN: 500Pa FN/500Pa Coll, 30kPa Coll-FN: 30kPa Coll/30kPa FN, 30kPa-HA Coll: 30kPa Coll/HA Coll, 30kPa-HA FN: 30kPa FN/HA FN, Glass-30kPa Coll: Glass/30kPa Coll, Glass-30kPa FN: Glass/30kPa FN). (N) refers to non-malignant (normal) cell lines. ***p-value < 0.01; **p-value < 0.05; *p-value < 0.1, adjusted for multiple testing using Benjamini-Hochberg procedure. For each cell line, phenotypic sensitivity to substrate change is calculated only if there are at least 25 data points ($n \geq 25$) for the physical feature of interest on both the substrates. See supplementary tables 1 and 2 for the exact value of n for the cell lines.



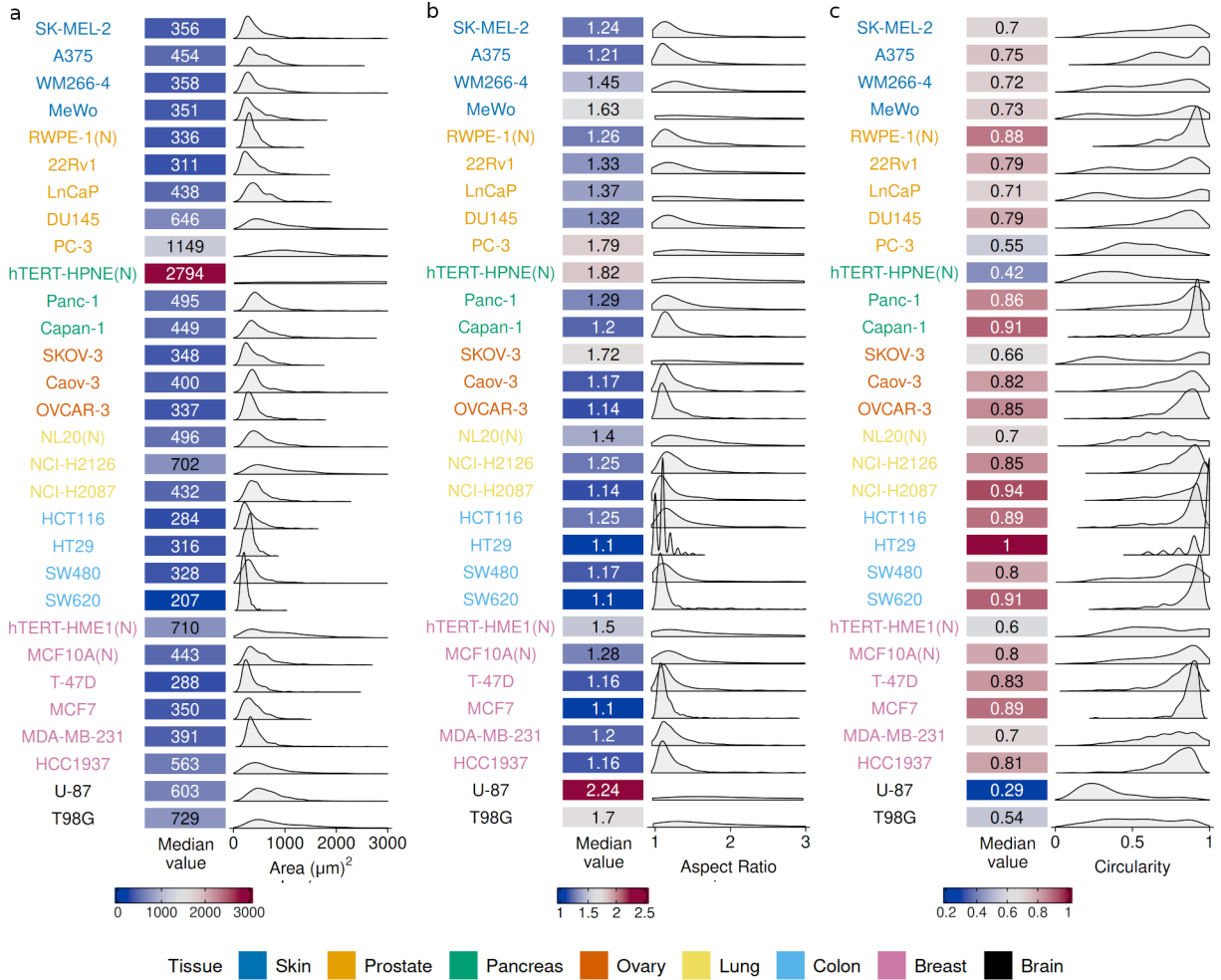
Supplementary Figure 3: For each cell line, the ratio of the median values for cell speed as a measure of the phenotypic sensitivity to substrate change. (HA Coll-FN: HA Coll/HA FN, 500Pa Coll-FN: 500Pa FN/500Pa Coll, 30kPa Coll-FN: 30kPa Coll/30kPa FN, 30kPa-HA Coll: 30kPa Coll/HA Coll, 30kPa-HA FN: 30kPa FN/HA FN, Glass-30kPa Coll: Glass/30kPa Coll, Glass-30kPa FN: Glass/30kPa FN). (N) refers to non-malignant (normal) cell lines. ***p-value < 0.01; **p-value < 0.05; *p-value < 0.1, adjusted for multiple testing using Benjamini-Hochberg procedure. For each cell line on a particular substrate, $n \geq 25$ cells. See supplementary tables 3 for the exact value of n for the cell lines.



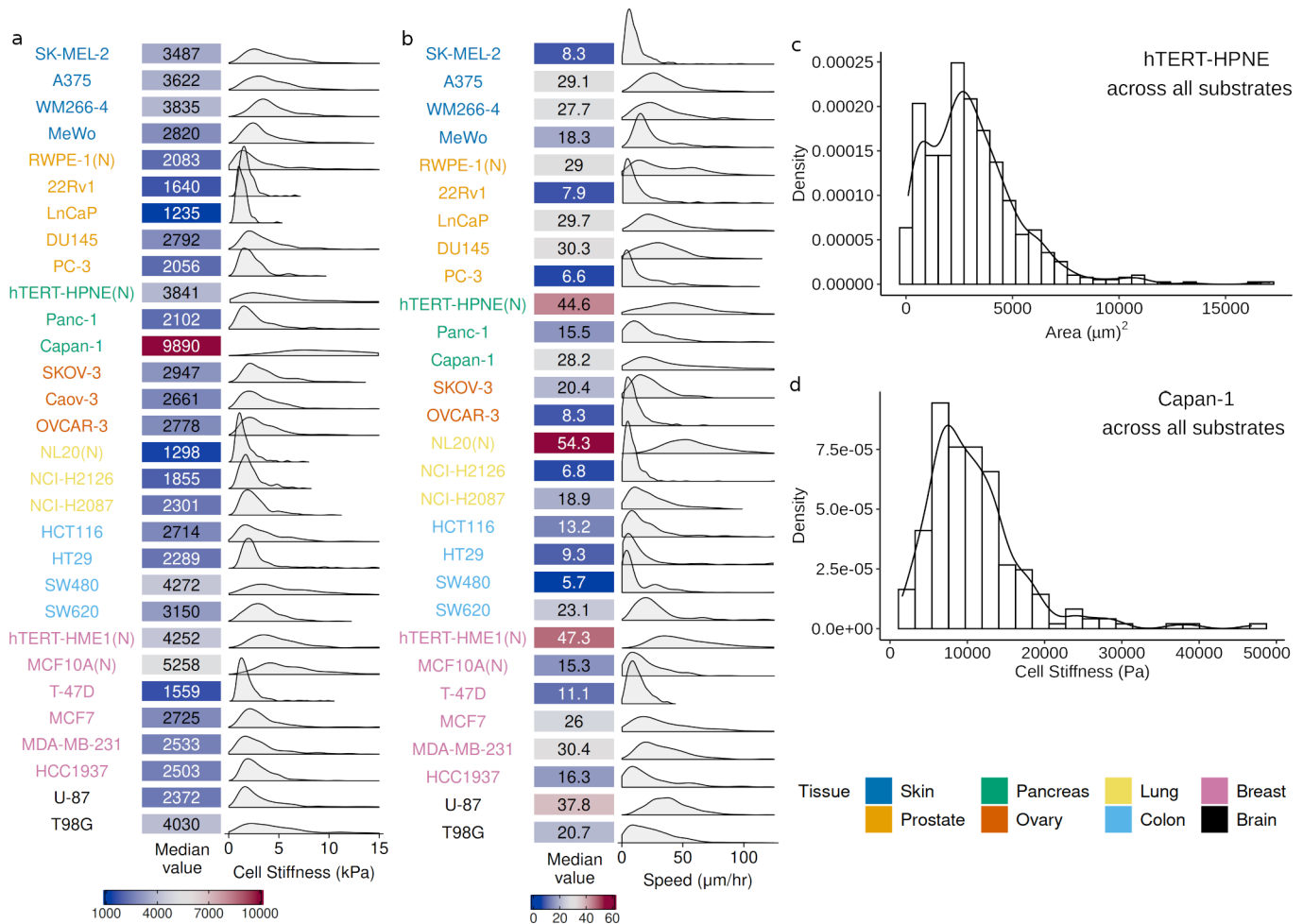
Supplementary Figure 4: For each cell line, the ratio of the median values for aspect ratio as a measure of the phenotypic sensitivity to substrate change. (30k-500Pa Coll: 30kPa Coll/500Pa Coll, 30k-500Pa FN: 30kPa FN/500Pa FN, HA-500Pa Coll: HA Coll/500Pa Coll, HA-500Pa FN: HA FN/500Pa FN, Glass-30kPa Coll: Glass/30kPa Coll, Glass-30kPa FN: Glass/30kPa FN, HA Coll-FN: HA Coll/HA FN, 500Pa Coll-FN: 500Pa FN/500Pa Coll, 30kPa Coll-FN: 30kPa Coll/30kPa FN, 30kPa-HA Coll: 30kPa Coll/HA Coll, 30kPa-HA FN: 30kPa FN/HA FN). (N) refers to non-malignant (normal) cell lines. ***p-value < 0.01; **p-value < 0.05; *p-value < 0.1, adjusted for multiple testing using Benjamini-Hochberg procedure. For each cell line on a particular substrate, $n \geq 25$ cells. See supplementary tables 1 for the exact value of n for the cell lines.



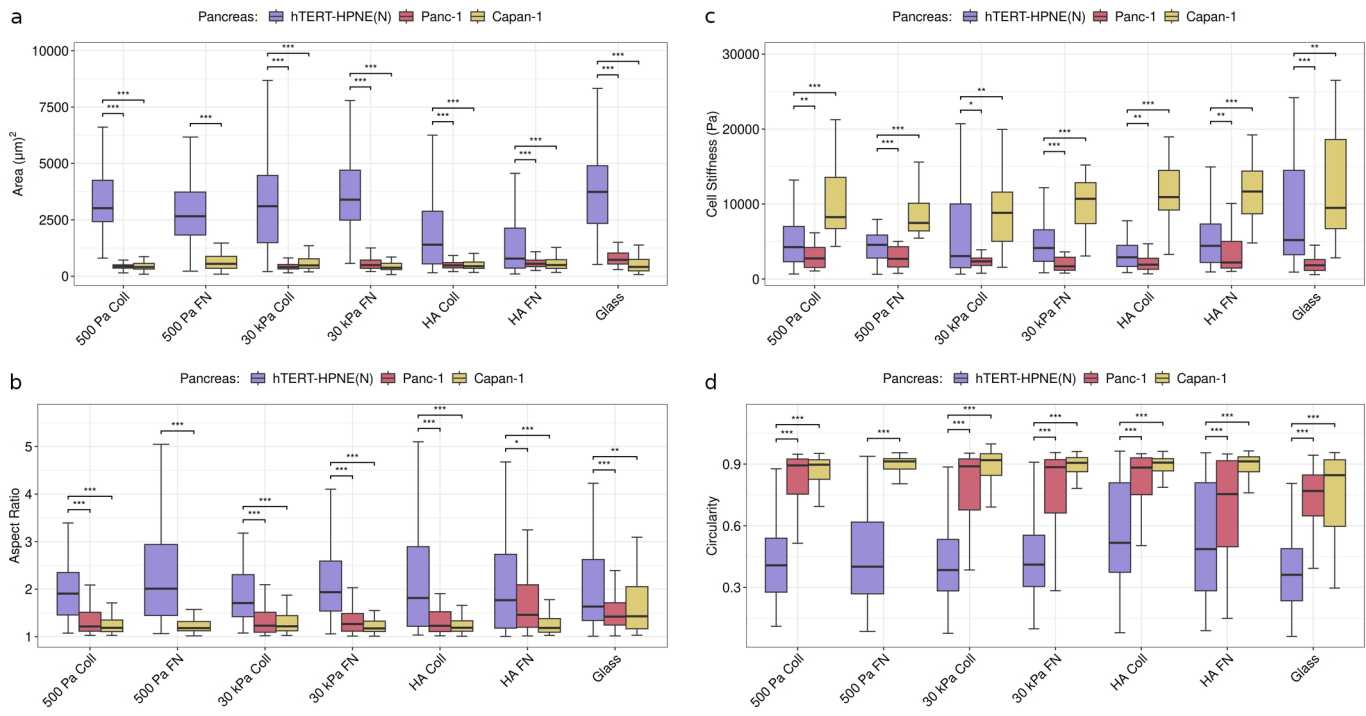
Supplementary Figure 5: For each cell line, the ratio of the median values for circularity as a measure of the phenotypic sensitivity to substrate change. (30k-500Pa Coll: 30kPa Coll/500Pa Coll, 30k-500Pa FN: 30kPa FN/500Pa FN, HA-500Pa Coll: HA Coll/500Pa Coll, HA-500Pa FN: HA FN/500Pa FN, Glass-30kPa Coll: Glass/30kPa Coll, Glass-30kPa FN: Glass/30kPa FN, HA Coll-FN: HA Coll/HA FN, 500Pa Coll-FN: 500Pa FN/500Pa Coll, 30kPa Coll-FN: 30kPa Coll/30kPa FN, 30kPa-HA Coll: 30kPa Coll/HA Coll, 30kPa-HA FN: 30kPa FN/HA FN). (N) refers to non-malignant (normal) cell lines. ***p-value < 0.01; **p-value < 0.05; *p-value < 0.1, adjusted for multiple testing using Benjamini-Hochberg procedure. For each cell line on a particular substrate, $n \geq 25$ cells. See supplementary tables 1 for the exact value of n for the cell lines.



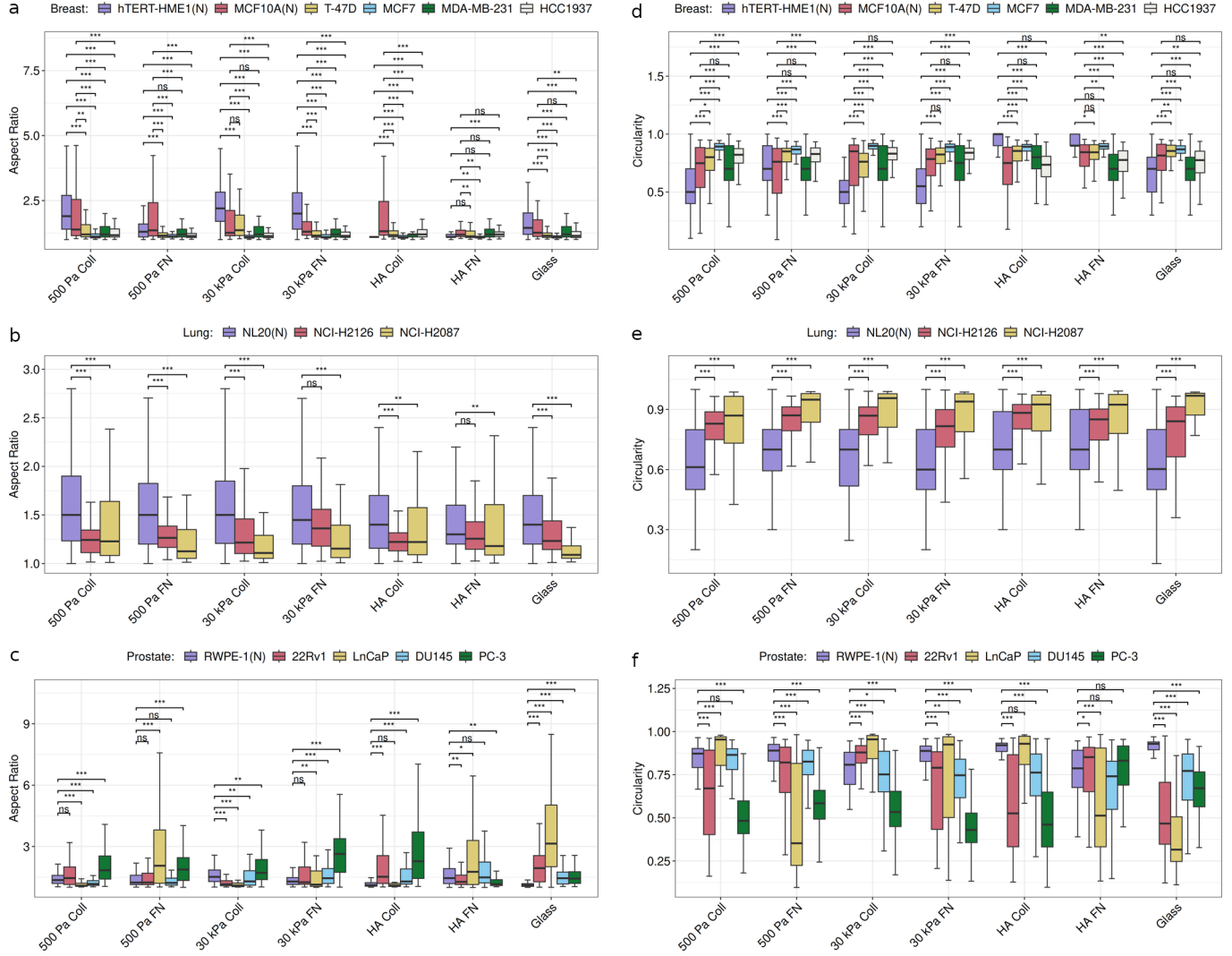
Supplementary Figure 6: Median values of cell (a) area, (b) aspect ratio, and (c) circularity across all the 7 different substrates, along with the kernel density estimates (KDE) for summarizing the distribution of feature values for each cell line. (N) refers to non-malignant (normal) cell lines. See supplementary figure 7c for the KDE of outlier-like distributions of hTERT-HPNE cellular area across all substrates.



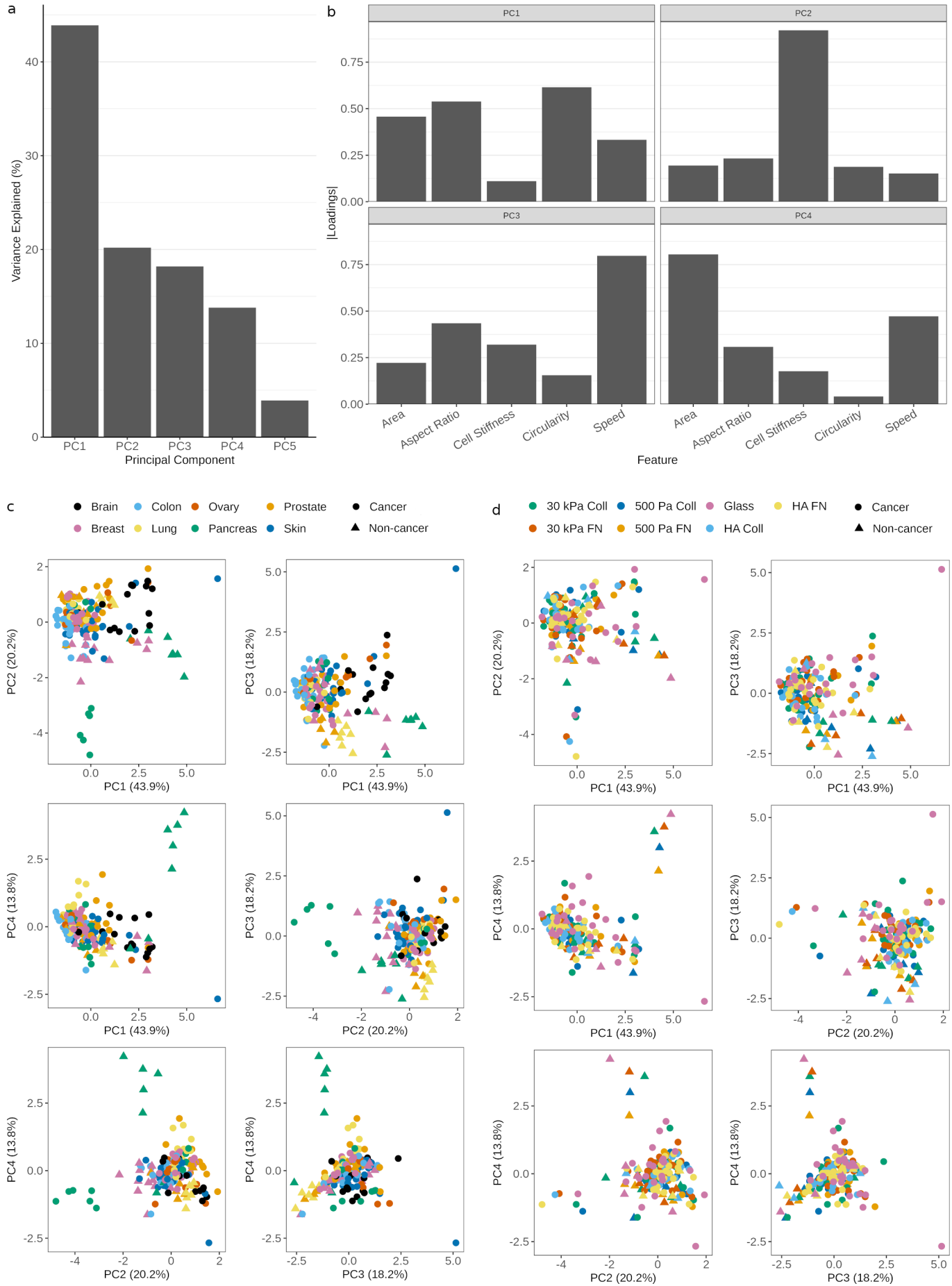
Supplementary Figure 7: Median values of (a) cell stiffness and (b) cell speed across all the 7 different substrates, along with the kernel density estimates (KDE) for summarizing the distribution of feature values for each cell line. (N) refers to non-malignant (normal) cell lines. KDEs for outlier-like distributions of (c) hTERT-HPNE cellular area across all substrates, and (d) Capan-1 cell stiffness across all substrates.



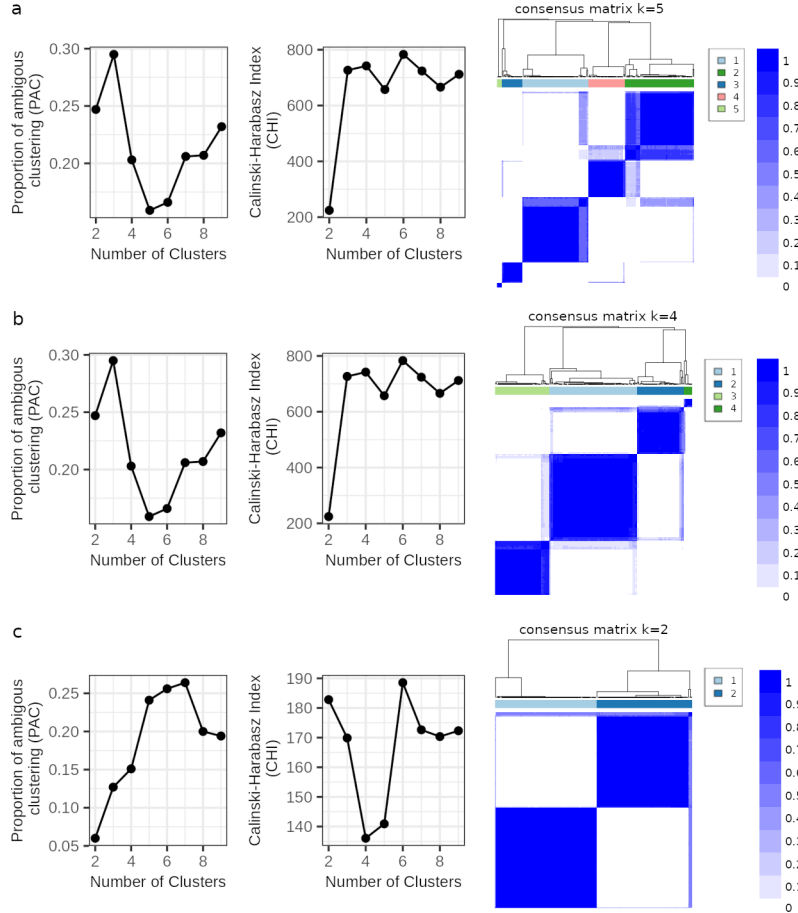
Supplementary Figure 8: Comparing tissue-specific normal and cancer cell behavior in terms of cell (a) area, (b) aspect ratio, (c) stiffness, and (d) speed for pancreatic cell lines soft (500 Pa) and stiff (30 kPa) PAAm Coll and FN substrates, soft (500 Pa) HA substrates coated with Coll and FN, and glass. (N) refers to non-malignant (normal) cell lines. ***p-value < 0.01; **p-value < 0.05; *p-value < 0.1, adjusted for multiple testing using Benjamini-Hochberg procedure. The number of measurements for the physical feature of interest is at least 25 ($n \geq 25$) for each cell line on a particular substrate. See supplementary tables 1-3 for the exact value of n for the cell lines.



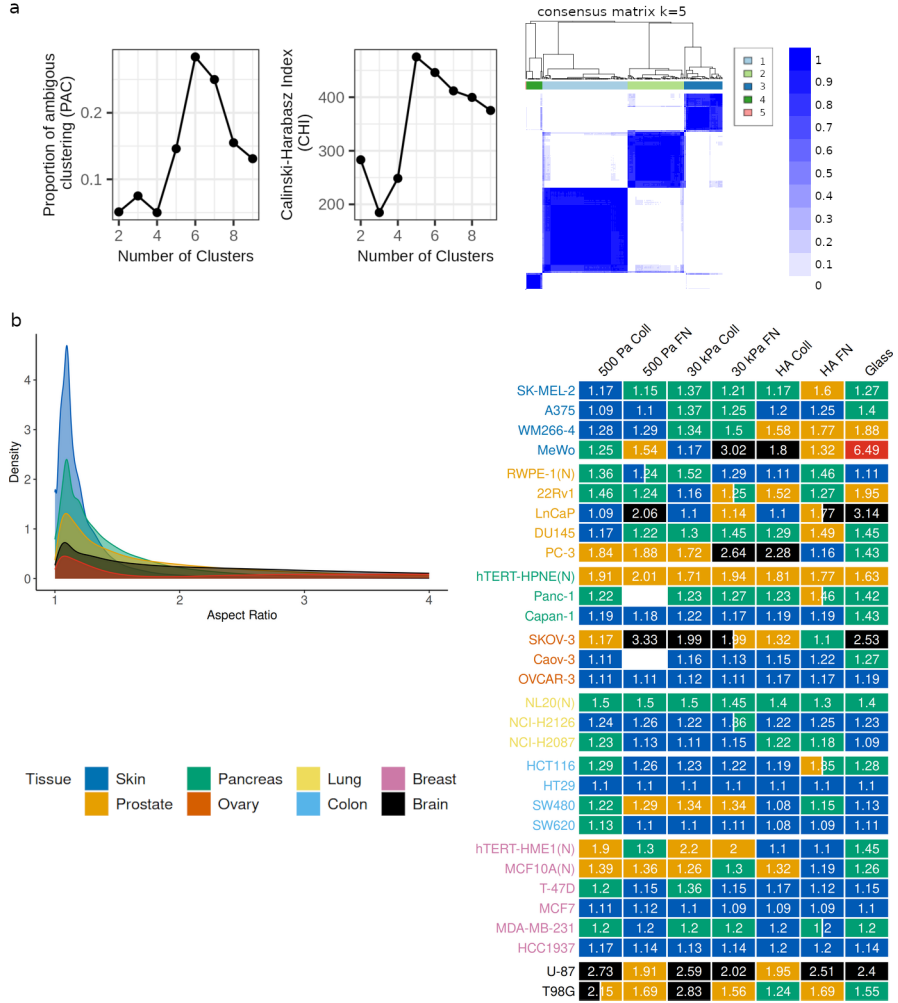
Supplementary Figure 9: Comparing tissue-specific normal and cancer cell behavior in terms of aspect ratio, and circularity for (a) breast, (b) lung, and (c) prostate cell lines soft (500 Pa) and stiff (30 kPa) PAAm Coll and FN substrates, soft (500 Pa) HA substrates coated with Coll and FN, and glass. (N) refers to non-malignant (normal) cell lines. ***p-value < 0.01; **p-value < 0.05; *p-value < 0.1, adjusted for multiple testing using Benjamini-Hochberg procedure. For each cell line on a particular substrate, $n \geq 25$ cells. See supplementary tables 1 for the exact value of n for the cell lines.



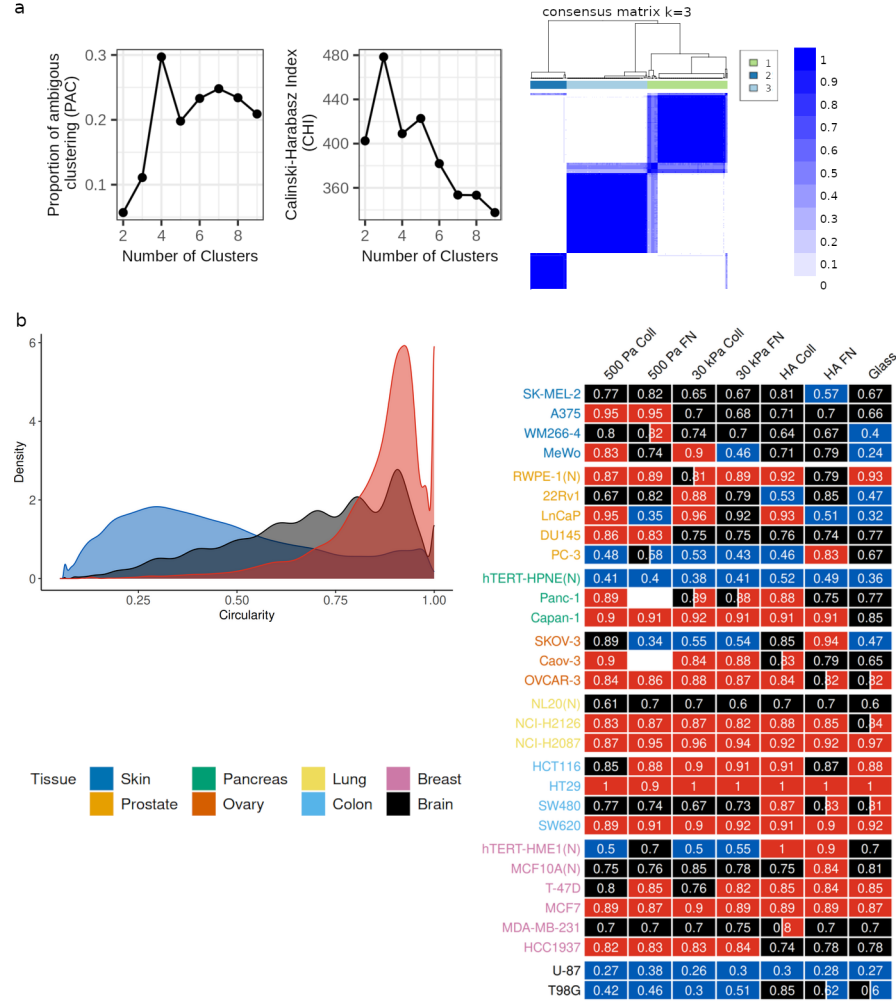
Supplementary Figure 10: Principal component analysis (PCA) performed using the median values of cell area, aspect ratio, circularity, stiffness, and speed from all the cell line-substrate pairs. Note that in this analysis only those cell line-substrate pairs are considered which have at least 25 data points for each of the physical feature. (a) Variance explained by each of the PCs, and (b) the loadings of the physical features on the first four PCs. Pairwise scatter plots for the first four PCs, with the points colored by the (c) tissue type and (d) substrate type.



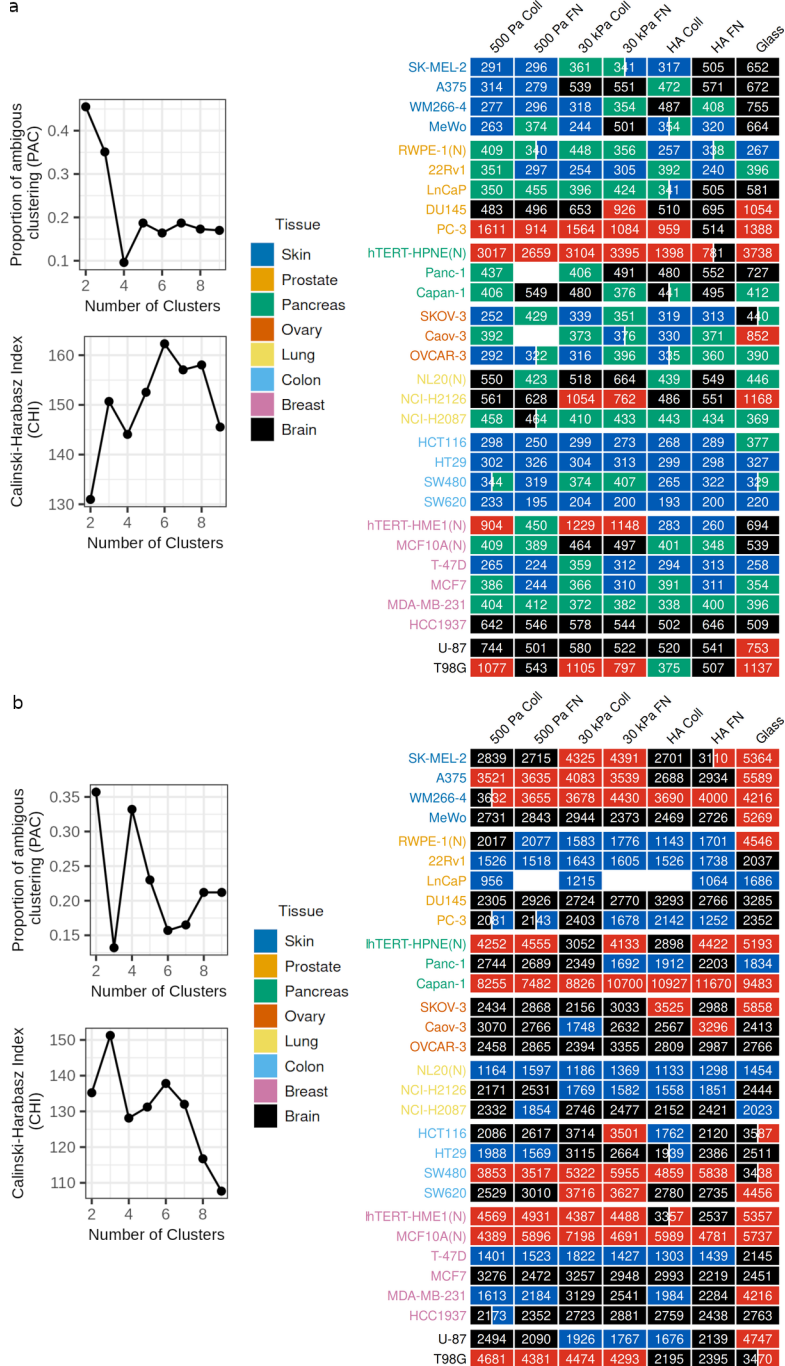
Supplementary Figure 11: Clustering statistics (PAC and CHI) used for identifying the optimal number of clusters (mechanotypes) based on Wasserstein-1 distance and the corresponding consensus matrix for optimal cluster count k of cell (a) area, (b) stiffness, and (c) speed.



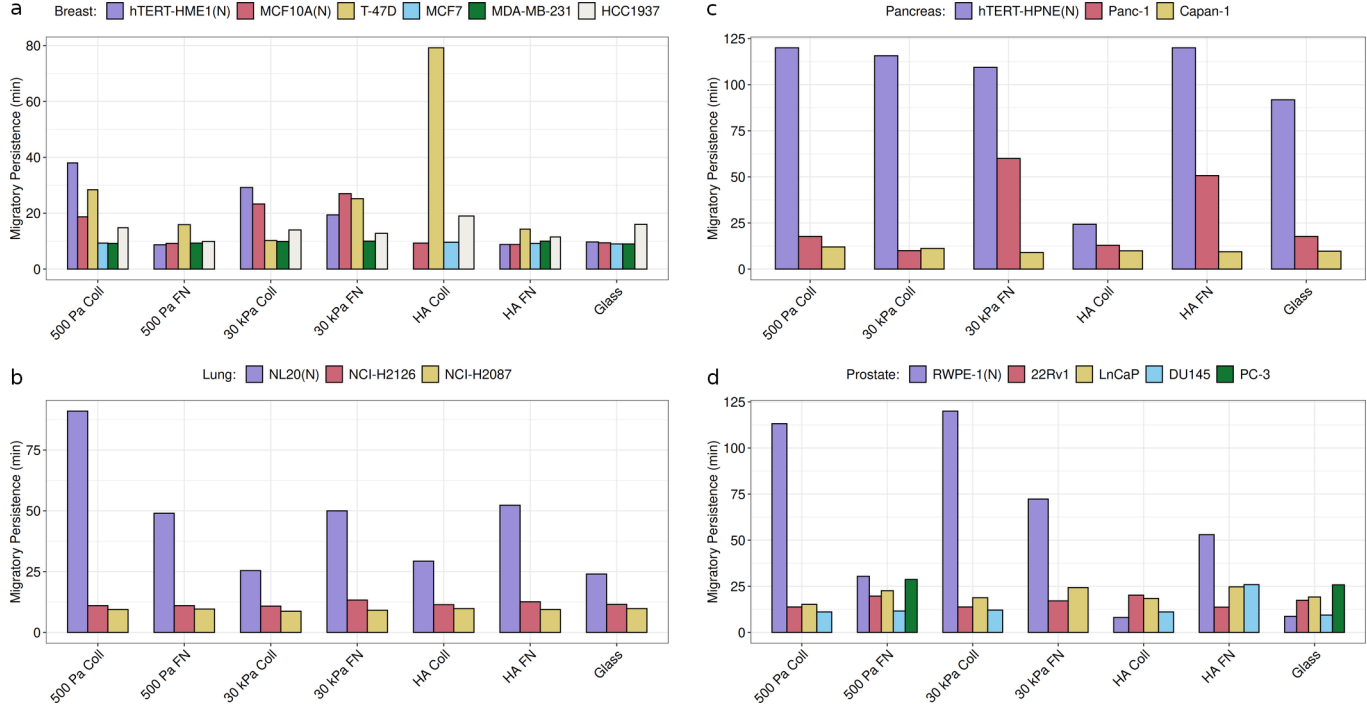
Supplementary Figure 12: (a) Clustering statistics (PAC and CHI) used for identifying the optimal number of clusters (mechanotypes) based on Wasserstein-1 distance and the corresponding consensus matrix for optimal cluster count k of circularity. (b) Mechanotypes for aspect ratio, whereby the heatmap shows the phenotypic class for each cell line-substrate pair and the KDEs correspond to characteristic density function for each class. The numeric values shown in the heatmap correspond to median values of circularity for each cell line-substrate pair. (N) refers to non-malignant (normal) cell lines. Note that in this analysis only those cell line-substrate pairs are considered which have at least 25 data points ($n \geq 25$) for the physical feature of interest. See supplementary tables 1 for the exact value of n for the cell lines.



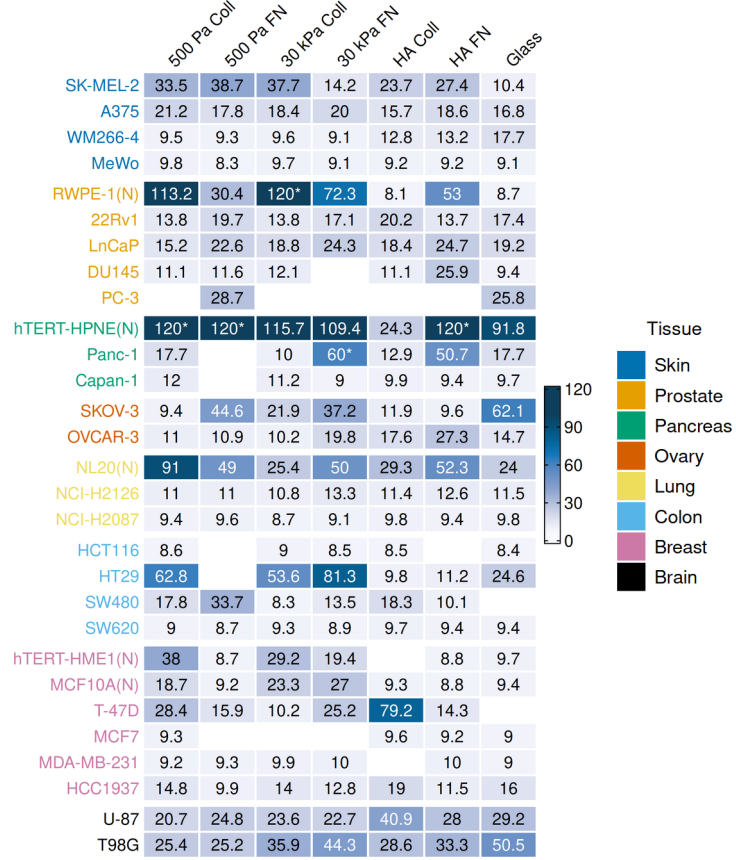
Supplementary Figure 13: (a) Clustering statistics (PAC and CHI) used for identifying the optimal number of clusters (mechanotypes) based on Wasserstein-1 distance and the corresponding consensus matrix for optimal cluster count k of circularity. (b) Mechanotypes for circularity, whereby the heatmap shows the phenotypic class for each cell line-substrate pair and the KDEs correspond to characteristic density function for each class. The numeric values shown in the heatmap correspond to median values of circularity for each cell line-substrate pair. (N) refers to non-malignant (normal) cell lines. Note that in this analysis only those cell line-substrate pairs are considered which have at least 25 data points ($n \geq 25$) for the physical feature of interest. See supplementary tables 1 for the exact value of n for the cell lines.



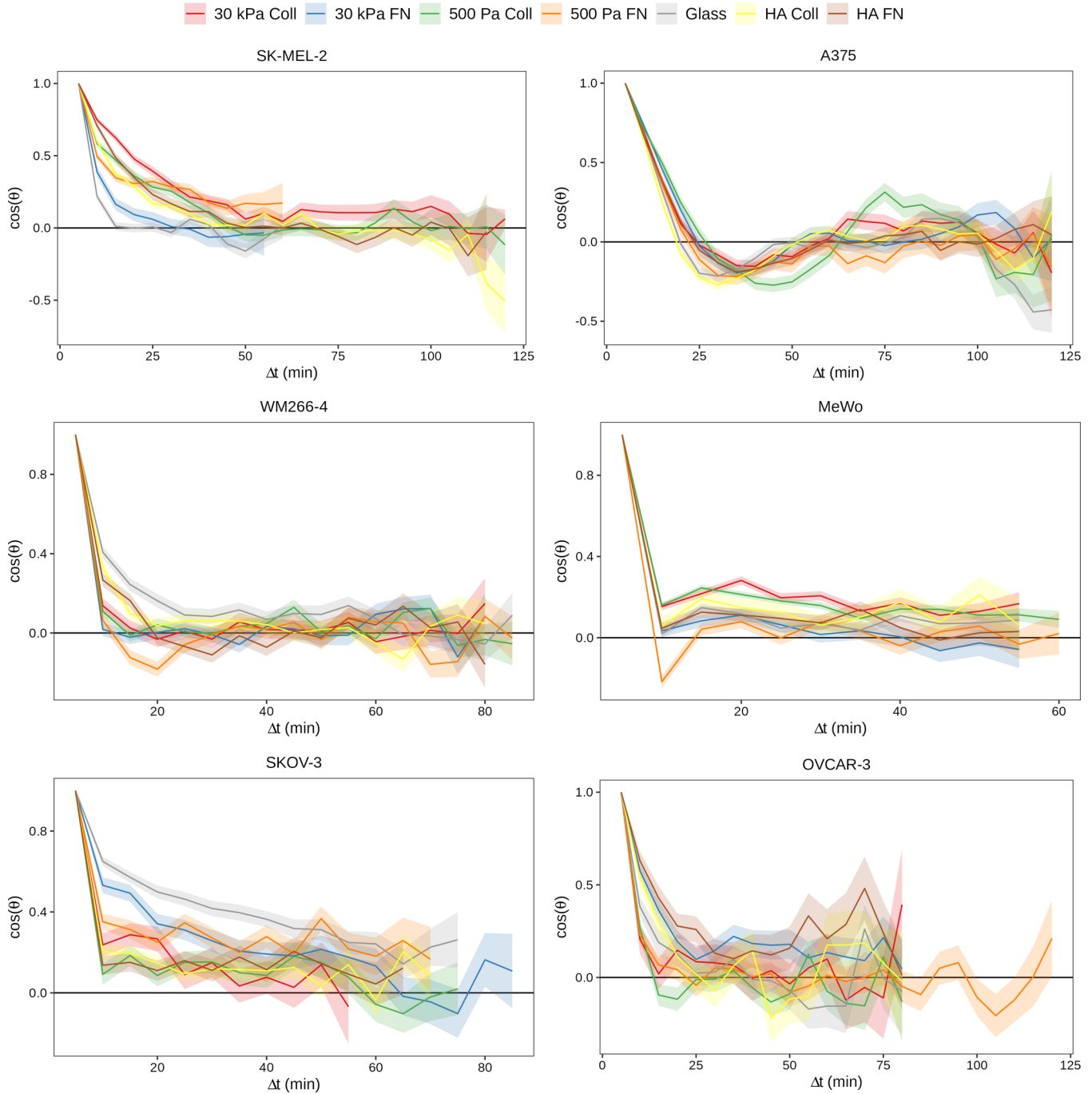
Supplementary Figure 14: Clustering statistics (PAC and CHI) used for identifying the optimal number of clusters based on Kolomogrov-Smirnov distance and the heatmap showing the corresponding classes for each of the cell line-substrate pairs for cell (a) area, and (b) stiffness. The numeric values shown in the heatmap correspond to median values of circularity for each cell line-substrate pair. (N) refers to non-malignant (normal) cell lines. Note that in this analysis only those cell line-substrate pairs are considered which have at least 25 data points ($n \geq 25$) for the physical feature of interest. See supplementary tables 1 and 2 for the exact value of n for the cell lines.



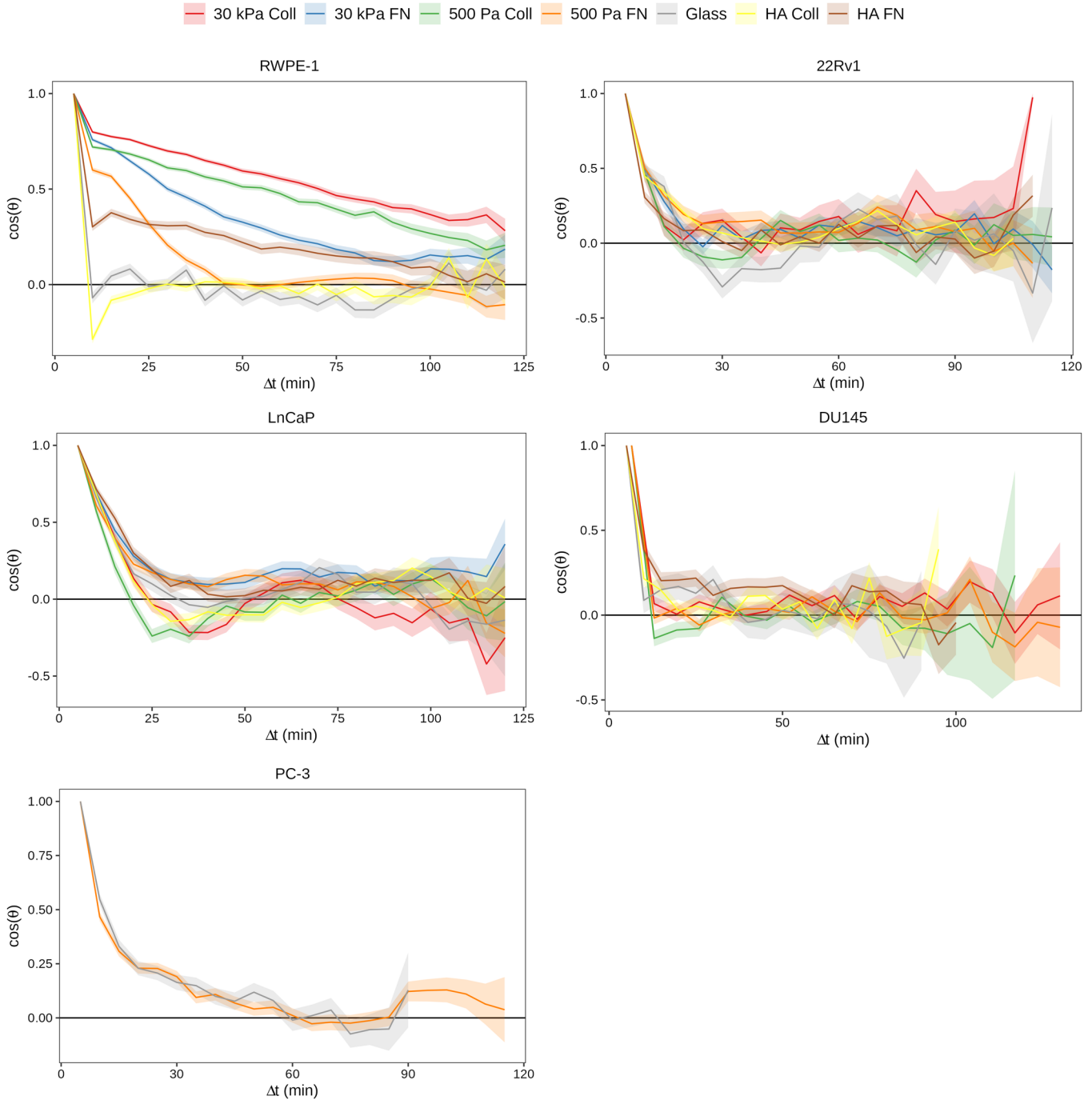
Supplementary Figure 15: Comparison between tissue-specific normal and cancer cell behavior in terms of migratory persistence for (a) breast, (b) lung, (c) pancreas, and (d) prostate cell lines. (N) refers to non-malignant (normal) cell lines. Decorrelation time estimated from directional autocorrelation curves (shown in Supp. Fig. 18-20) is used as a measure of migratory persistence. Note that, for RWPE-1 cell line on 30 kPa Coll, hTERT-HPNE cell line on 500 Pa Coll, 500 Pa FN and HA FN, and Panc-1 cell line on 30 kPa FN, the directional autocorrelation did not fall below 0.2 cutoff used to determine decorrelation time. For these cases, the total trajectory time is used as a measure of migratory persistence.



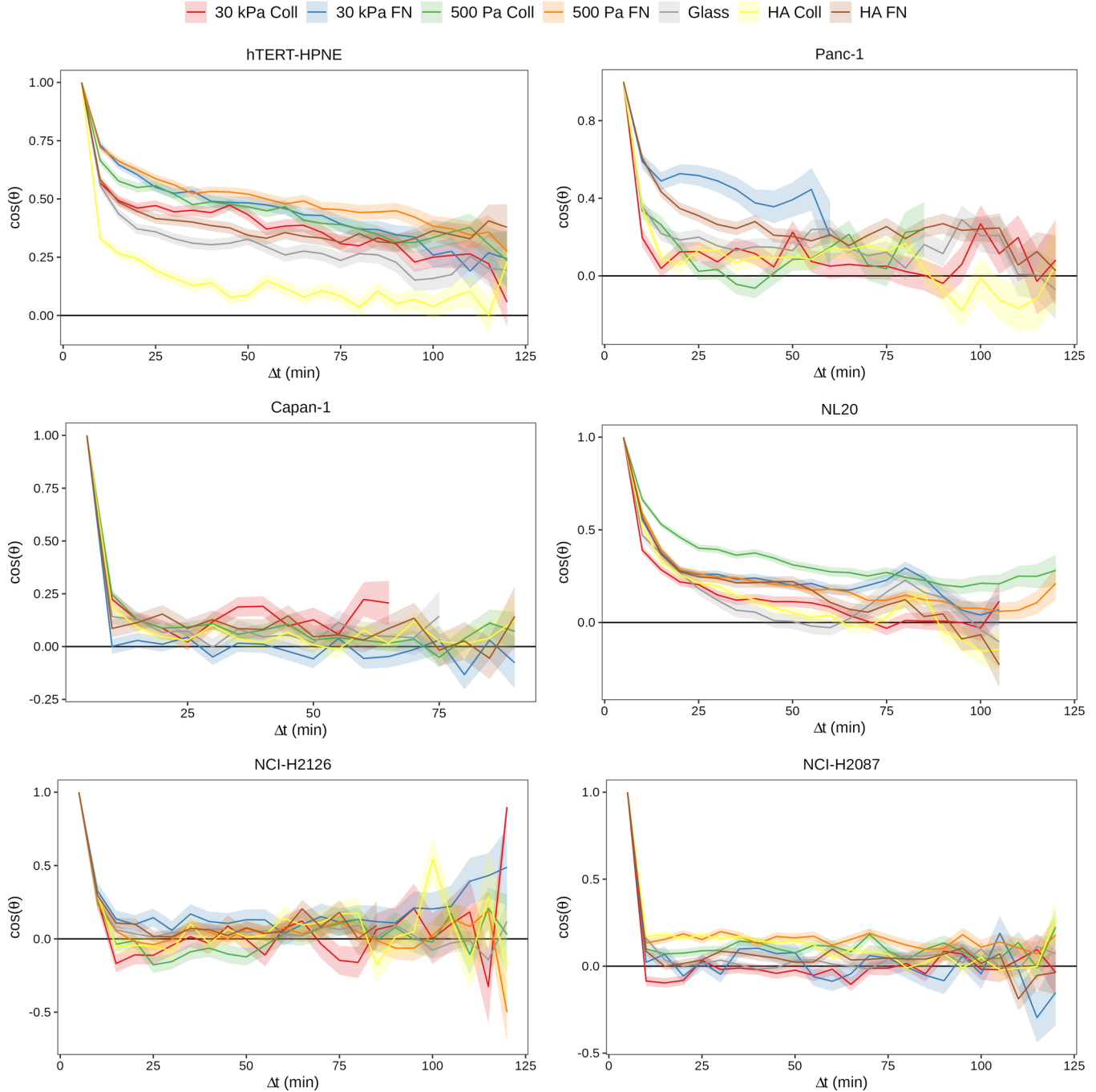
Supplementary Figure 16: Heatmap showing the migratory persistence for each of the cell line-substrate pairs. (N) refers to non-malignant (normal) cell lines. Decorrelation time estimated from directional autocorrelation curves (shown in Supp. Fig. 17-21) is used as a measure of migratory persistence. Note that (*) represents the cell line-substrate pairs for which the directional autocorrelation did not fall below 0.2 cutoff used to determine decorrelation time. For these cases, the total trajectory time is used as a measure of migratory persistence.



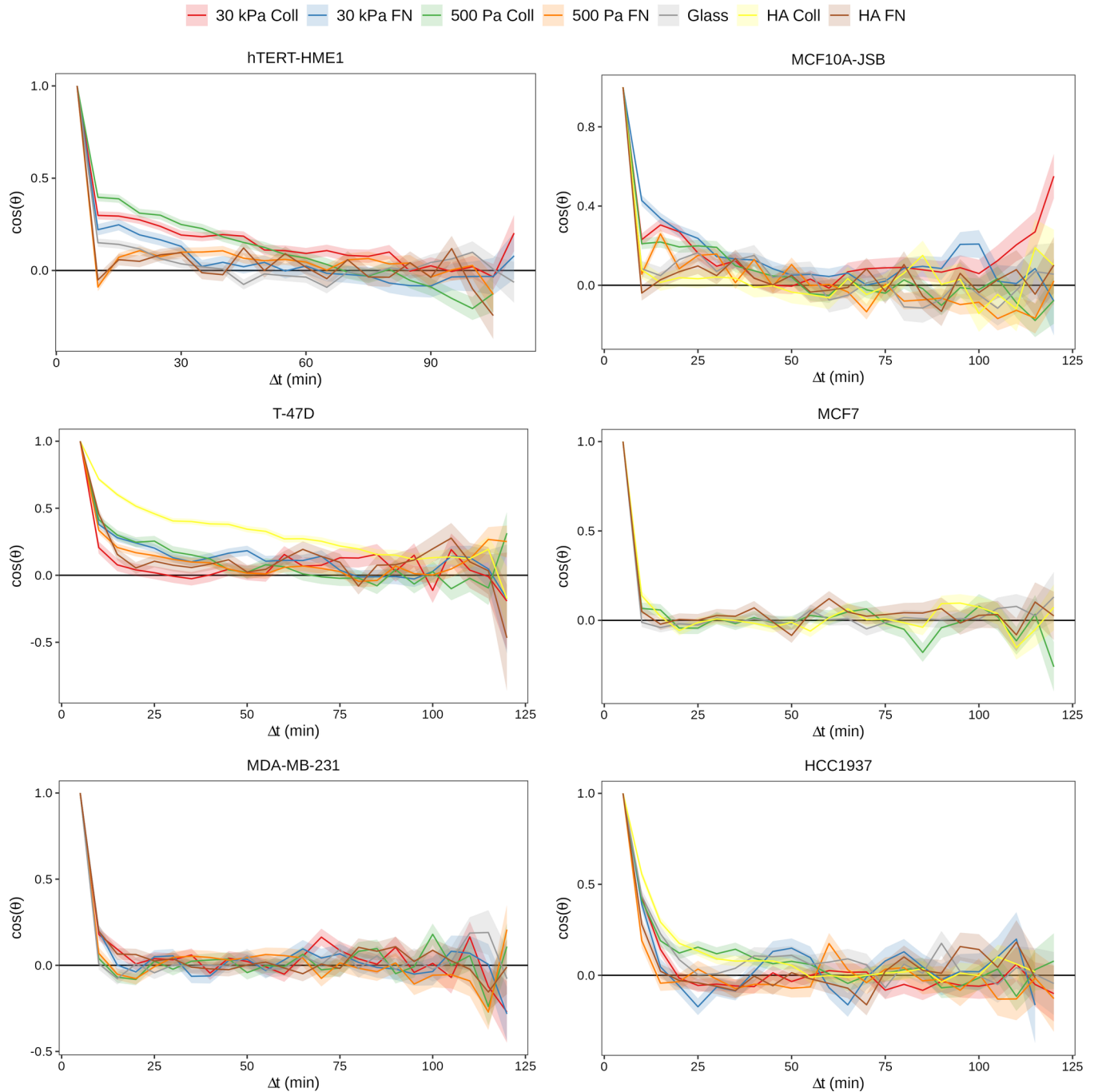
Supplementary Figure 17: Directional autocorrelation comparing the persistence of cell migration for cell lines on different substrates. For each cell line, only those substrates are analysed that have $n \geq 25$ measurements. See supplementary tables 3 for the exact value of n for the cell lines.



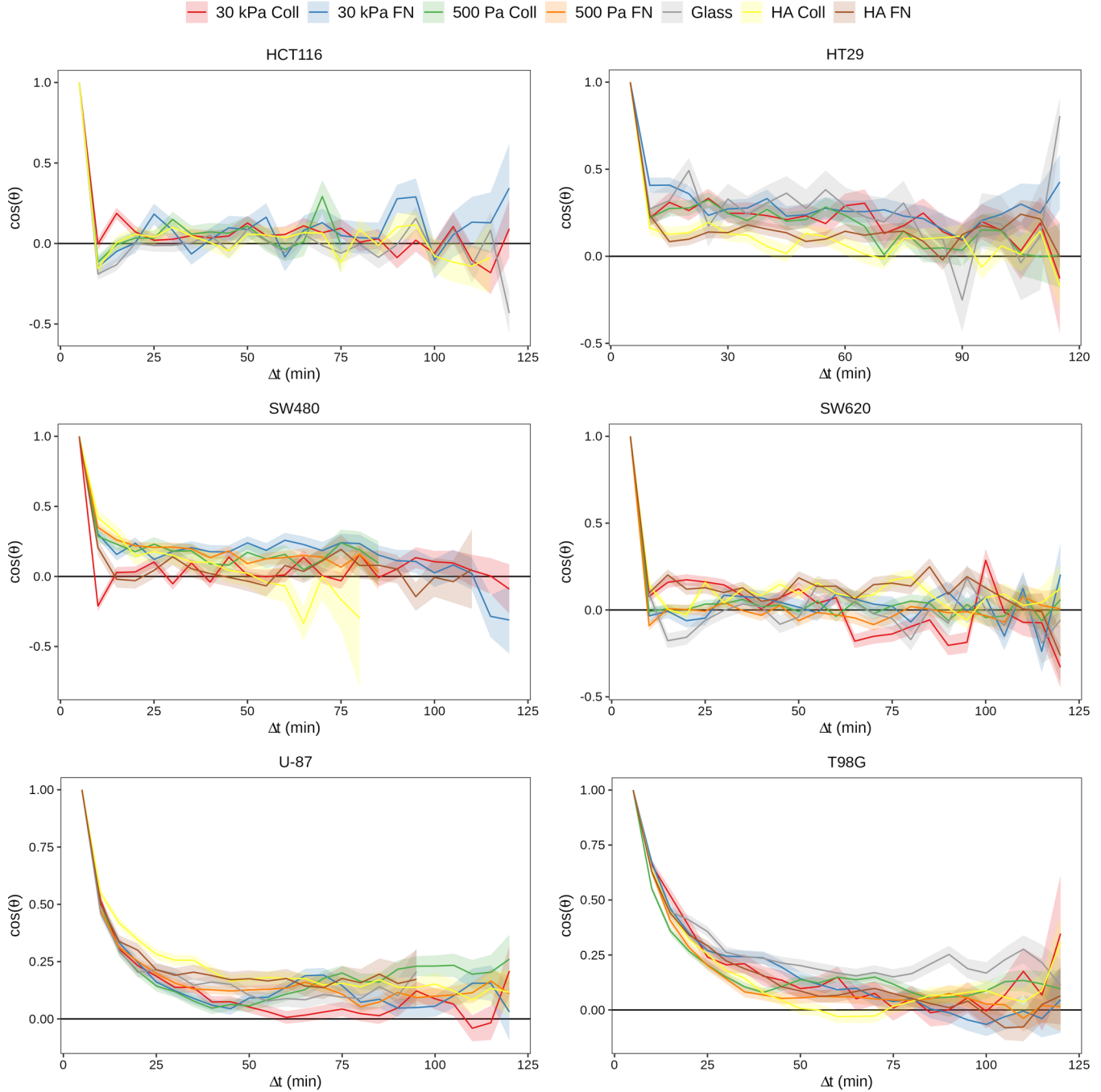
Supplementary Figure 18: Directional autocorrelation comparing the persistence of cell migration for cell lines on different substrates. For each cell line, only those substrates are analysed that have $n \geq 25$ measurements. See supplementary tables 3 for the exact value of n for the cell lines.



Supplementary Figure 19: Directional autocorrelation comparing the persistence of cell migration for cell lines on different substrates. For each cell line, only those substrates are analysed that have $n \geq 25$ measurements. See supplementary tables 3 for the exact value of n for the cell lines.



Supplementary Figure 20: Directional autocorrelation comparing the persistence of cell migration for cell lines on different substrates. For each cell line, only those substrates are analysed that have $n \geq 25$ measurements. See supplementary tables 3 for the exact value of n for the cell lines.



Supplementary Figure 21: Directional autocorrelation comparing the persistence of cell migration for cell lines on different substrates. For each cell line, only those substrates are analysed that have $n \geq 25$ measurements. See supplementary tables 3 for the exact value of n for the cell lines.